Migration of point defects and a defect pair in zinc oxide using the dimer method

Dong Chen
Department of Physics and Electronics, Institute of Photo-biophysics, Henan University, Kaifeng 475004, China

Fei Gao[a)]
Pacific Northwest National Laboratory, Richland, Washington 99352

Mingdong Dong
Interdisciplinary Nanoscience Center (iNANO), University of Aarhus, Ny Munkegade, DK-8000, Aarhus C, Denmark

Bo Liu[b)]
Department of Physics and Electronics, Institute of Photo-biophysics, Henan University, Kaifeng 475004, China

(Received 13 February 2012; accepted 4 April 2012)

The migration mechanism and the minimum energy path of vacancies, interstitials, and an interstitial–vacancy pair in zinc oxide have been studied by the dimer method. The in-plane and out-of-plane migrations of zinc and oxygen vacancies are anisotropic. The kick-out mechanism is energetically preferred to zinc and oxygen interstitials that can easily migrate through the ZnO crystal lattice. In addition, the migration process of an interstitial–vacancy pair as a complex of an octahedral oxygen interstitial and a zinc vacancy is dominated by an oxygen interstitial/zinc vacancy successive migration. The energy barriers indicate that the existence of oxygen interstitial in the defect pair can promote the mobility of zinc vacancy, whereas the migration of oxygen interstitial is slowed down due to the presence of zinc vacancy. In the end, we show a possible migration path of the interstitial–vacancy pair that can be dissociated through a set of displacement movements.

I. INTRODUCTION

For the last few decades, zinc oxide has been under intensive investigation because of its potential applications in electronic, optoelectronic, semiconductor, and spintronic devices.[1,2] Particularly, the wurtzite structure composed of alternating planes, which are occupied by tetrahedrally coordinated O^{2-} and Zn^{2+} ions, largely enhances the piezoelectricity and pyroelectricity properties of ZnO. Furthermore, point defects and impurities during the crystal growing process significantly influence the structural and electronic properties of materials. Therefore, knowledge of migration behaviors of point defects in ZnO material is essential to control the formation of native point defects and explore novel application fields. A large amount of literature in this area has already been published.[3–6] Oxygen vacancy, zinc interstitial, and zinc Frenkel pairs in ZnO have been studied by electron paramagnetic resonance.[7,8] A detailed study of the electronic and structural properties and stability of all native point defects in ZnO was performed by first-principles methods.[9] Erhart and Albe[10,11] determined the migration paths of intrinsic defects in ZnO by using density functional calculations combined with the climbing image nudged elastic band (NEB) method. Defect clusters in ZnO could give valuable insights into the dynamics of microstructural change in materials and point defect incorporation and dissociation, whereas isolated defects show a high tendency to form defect complexes by combining with other defects under radiation damage conditions. However, experimental information about defect cluster migration in ZnO is ambiguously interpretable on the atomic scale. Since the influence of defect clusters on structural properties of ZnO is still controversial partly because of a lack of theoretical studies, computer simulations may provide important insights into the migration behaviors of point defects and defect clusters in ZnO.

The NEB[12] and the dimer[13] methods have been widely used to search for minimum energy paths (MEPs) of the migrations of defects and defect clusters in materials. For a given initial and final state of a transition, the MEP is easily found using the NEB method. However, it is very challenging to find the MEP for the transition, if the final state or the mechanism of transition is unknown. The dimer method is an independent implementation of hybrid eigenvector following approach[14] and was developed by Henkelman and Jónsson. Compared to the NEB method,

Address all correspondence to these authors.
[a)]e-mail: fei.gao@pnl.gov,
[b)]e-mail: boliu@henu.edu.cn.
DOI: 10.1557/jmr.2012.153

 © Materials Research Society 2012

https://doi.org/10.1557/jmr.2012.153 Published online by Cambridge University Press

the dimer technique is an especially useful tool for a cluster when the lowest energy final state of its transition is not easily predictable. This method has been used to study possible transition states of defects in SiC and α-Fe,[15] the migration behaviors of tungsten clusters on nanoparticle,[16] and Cr-vacancy clusters in α-Fe.[17]

In this paper, we have used the dimer method to probe possible transition states, MEPs, and migration mechanisms of vacancies, interstitials, and an interstitial-vacancy pair in zinc oxide. The migrations of zinc and oxygen interstitials occur by a kick-out mechanism and are energetically preferred over the vacancies. Finally, we devote more attention to an interstitial–vacancy pair as a complex consisting of an octahedral oxygen interstitial and a zinc vacancy and explore how a vacancy affects the migration behavior of an I_O during the migration processes.

II. DETAILS OF THE CALCULATION

In each configuration, the force calculations were carried out by using version 2.19 of the DL_POLY package.[18] The computational cell of wurtzite structure consisted of 7 × 7 × 7 unit cells containing 1372 atoms. Three-dimensional periodic boundary conditions were applied and calculations were carried out at constant volume. We use the Buckingham potential for ZnO to describe the atomic interaction with parameters previously published by Kulkarni et al.[19] This potential has been widely used to simulate defect and monovalent ion incorporation, to produce the wurtzite crystalline lattice parameters, and also to predict elastic and mechanical properties of ZnO nanostructures.[19–21] The long-range Coulomb force was considered by using the smoothed particle mesh Ewald method with a cutoff distance of 10 Å. The van der Waals cutoff distance chosen in the simulations was 10 Å.

The possible transition states and migration paths of defects are determined by the dimer method. In the dimer method, the saddle point search is completed through moving the dimer on the potential energy surface (PES), which is the 3N-dimensional surface of all possible configurations of the N atoms in the system, from the vicinity of the potential energy minimum of the initial state up to a saddle point. Basins of the PES are stable states, while saddle points correspond to the lowest energy transition points between states, from which the

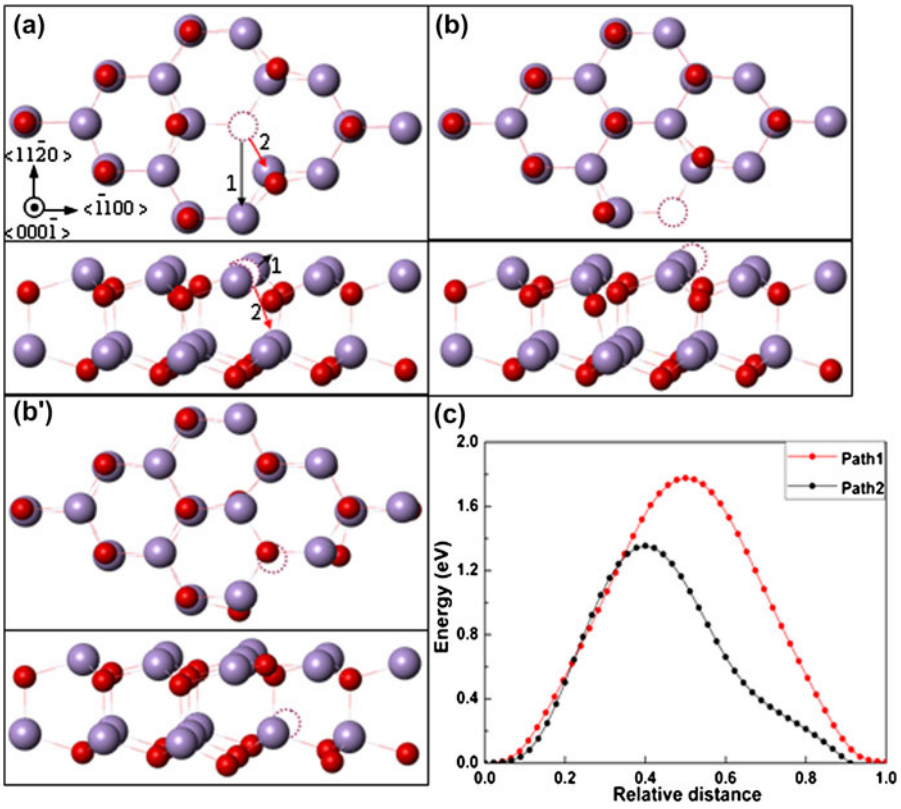


FIG. 1. Migration paths and calculated energy paths that correspond to this migration process of a zinc vacancy. (a) Starting configuration, (b) and (b′) two possible final configurations, and (c) calculated energy barriers corresponding to path 1 (a→b) and path 2 (a→b′). The red and light purple spheres represent the O atoms and Zn atoms, respectively. Also the dotted light purple circle indicates the zinc vacancy. Upper panels show top views, while lower panels show side views. Side views are perpendicular to the <0001> direction and top views are along the <000$\bar{1}$> direction. In the first frame, the respective paths are labeled. The arrow indicates the vacancy movement at the next step.

https://doi.org/10.1557/jmr.2012.153 Published online by Cambridge University Press

minimum energy barrier for a transition to take place can be determined. Thus, during the search, each time the dimer is displaced; it is also rotated to find the minimum energy configuration. Once the saddle points for the transitions involved in defect migration are determined, it is possible to trace out the MEPs. For each initial configuration, we carried out 100 dimer searches with different initial random vectors that have nonzero components only for a 20–30-atom subset of the system near the defect, which allows the system to be displaced from a distribution of nearly equal potential energy minima in the initial basin. The dimer separation was set at 1×10^{-4} Å, and the values of the finite difference steps for rotation and translation were 10^{-4} and 10^{-3} Å, respectively. The maximum move distance was set at 0.15 Å and the search was stopped when the maximum force of atoms became less than 0.01 eV/Å.

III. RESULTS AND DISCUSSION

A. Migration of zinc vacancy

First-principles calculations[22,23] have revealed that the migration of zinc vacancy occurs when the nearest neighbor atom directly jumps into the vacancy site. Here, we show two typical migration processes of a zinc vacancy that may occur in the wurtzite-structured ZnO.

The MEPs of a single zinc vacancy (V_{Zn}) using the dimer method and the corresponding processes are shown in Fig. 1. As expected, the common migration mechanism is the nearest neighbor Zn atom jumping into the vacancy position with the energy barrier of 1.77 eV (a→b) and 1.35 eV (a→b′), respectively. For path 1, the nearest neighbor zinc atom in the same basal plane as the V_{Zn} jumps into the vacancy position, which corresponds to the position exchange of the Zn atom and vacancy (see a→b in Fig. 1). It is obvious that the energy curve of path 1 is symmetric and the middle point of the migration path is a saddle point. Path 2 occurs when a nearest neighbor zinc atom in the adjacent basal plane hops into the vacancy site (see a→b′ in Fig. 1). The energy barrier for this path is 1.35 eV and is about 0.43 eV lower than that for path 1. Taking into account the large deformation due to the Zn atom movement following path 1, it is expected that path 1 has a relatively high barrier. Both migration energies calculated for the V_{Zn} are reasonably consistent with first-principles calculations reported by Erhart and Albe.[10] These two migration processes demonstrate that the diffusion of a zinc vacancy in ZnO is anisotropic.

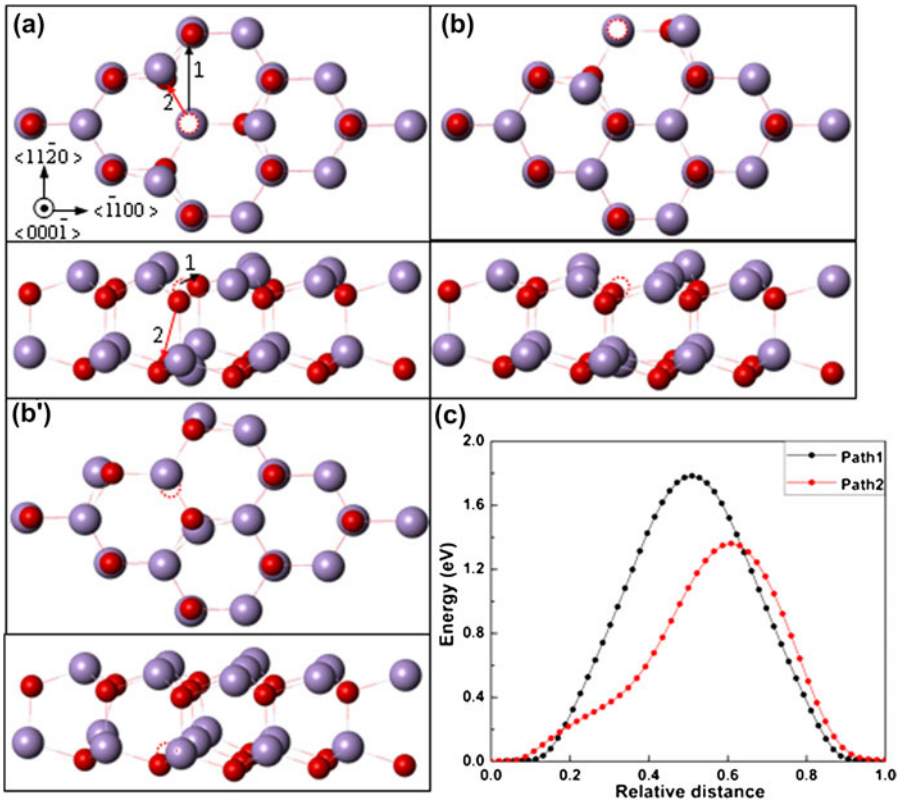


FIG. 2. Migration paths and calculated energy paths of an oxygen vacancy. (a) Starting configuration, (b) and (b′) two possible final configurations, and (c) calculated energy barriers corresponding to path 1 (a→b) and path 2 (a→b′). The dotted red circle indicates the oxygen vacancy.

https://doi.org/10.1557/jmr.2012.153 Published online by Cambridge University Press

B. Migration of oxygen vacancy

Similarly, the migration of an oxygen vacancy (V_O) occurs by a nearest neighbor O atom directly jumping to the vacancy site. The migration paths determined by the dimer search and the corresponding MEPs are shown in Fig. 2. The nearest neighbor oxygen atom in the same basal plane of V_O can directly move into the vacancy position (see a→b in Fig. 2), which leads to an energy barrier of 1.78 eV, similar to that of the V_{Zn} discussed above. Path 2 represents a transition of a nearest neighbor oxygen atom in the adjacent basal plane jumping to the vacancy site (see a→b′ in Fig. 2). This transition leads to a lower energy barrier of 1.36 eV, which is in agreement with the calculated value reported by Erhart and Albe.[11] In spite of the local geometry around the oxygen vacancy with tetrahedral symmetry, the migration of V_O also shows an anisotropic behavior based on our calculations, which is similar to the anisotropic migration behavior of the V_{Zn}, as discussed above. It should be pointed out that vacancy migration is unlikely to be a dominant migration process in ZnO, considering its higher energy barrier, and hence, a complex defect needs to be studied.

C. Migration of zinc interstitial

A zinc interstitial (I_{Zn}) is initially placed in an octahedral interstitial position in the wurtzite lattice, and the possible migration process is described in Fig. 3. The migration path shows that the I_{Zn} pushes out the nearest neighbor zinc atom, which then transfers to a new interstitial atom (see a→b→c in Fig. 3). In the case of a kick-out (or interstitialcy) mechanism, the dimer method results in an energy barrier of 0.76 eV as shown in Fig. 3(d). The midway along the migration path between initial and final states is the saddle point. At the saddle point, the two Zn atoms share a lattice site forming a rather symmetric configuration as shown in Fig. 3(b). Clearly, the Zn interstitial is quite mobile via overcoming a small energy barrier, which is 0.59 eV lower than that for the V_{Zn} migration (1.35 eV). Taking into account the low energy barrier of zinc interstitial, zinc interstitials may be trapped by other defects or impurities and diffuse with these defects together, which was proposed in Ref. 22.

D. Migration of oxygen interstitial

Of the 100 dimer searches for an oxygen interstitial (I_O) at the octahedral interstitial site, 12 searches converge

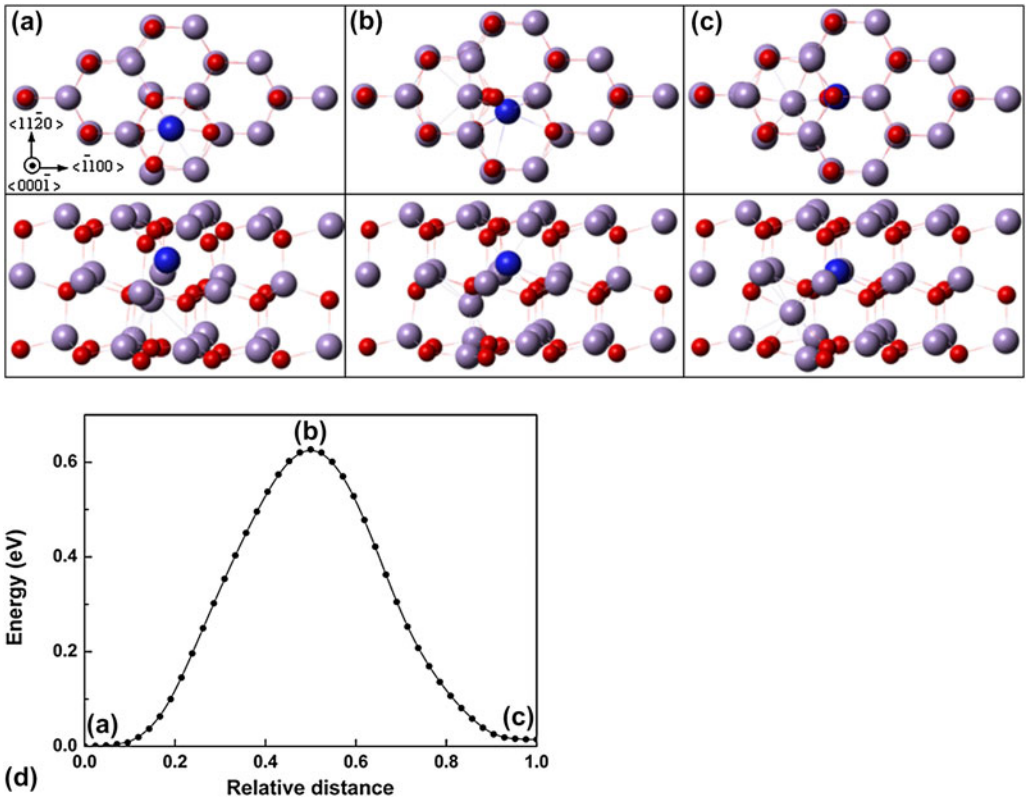


FIG. 3. The kick-out migration mechanism and the MEP of a zinc interstitial. (a) Starting configuration, (b) saddle point, (c) final configuration where a new zinc interstitial is formed in an adjacent basal plane, and (d) the calculated energy barrier. To easily follow the interstitial movements, we use the blue sphere to represent the initial zinc interstitial.

https://doi.org/10.1557/jmr.2012.153 Published online by Cambridge University Press

to a saddle point with an energy of 0.13 eV, 13 searches converge to other saddle points with the energies of 0.58–0.96 eV, 2 searches fail to find saddle points, some of 73 searches could not converge to the original initial state, and the others lead to physically improbable energy values. As shown in Fig. 4, three typical migration processes occur, one involving a slight displacement for the transform between two nonsymmetric configurations (see a→c in Fig. 4) and two being the kick-out mechanisms (see a→b′→c′ and a→b″→c″ in Fig. 4), respectively. In Fig. 4(d), we show the MEPs corresponding to these migration processes. After the lattice relaxation of the starting configuration, the oxygen atom at the first nearest neighbor lattice site moves away from its original lattice position about 0.95 Å along the <0001> direction. As illustrated in Fig. 4(a), the oxygen atom is noticeably pushed upwards due to the existence of the I_O. The similar nonsymmetric configuration of an oxygen interstitial was also found in the previous study.[24] The I_O slightly moves along the $<1\bar{1}00>$ direction and then pushed another oxygen atom at the lattice site upwards (see a→c in Fig. 4), which is easily understood from the side views in Figs. 4(a) and 4(c). The calculated migration barrier for path 1 (a→c) is 0.13 eV. However, the path 1 of the I_O only involves configuration transformation and is unlikely to contribute to the long distance migration behavior.

Both path 2 (a→b′→c′) and path 3 (a→b′′→c′′) display a similar kick-out mechanism, where the I_O moves close to a nearest neighbor oxygen atom, occupies the lattice site, and then pushes it toward the adjacent basal plane to form a new octahedral interstitial. The migration energy barrier for path 2 is determined to be 0.58 eV, which is comparable to that of the I_{Zn} migration in ZnO. Furthermore, the final state [see Fig. 4(c′)] is also a nonsymmetric configuration in which the original I_O is pushed upwards around 0.25 Å along the <0001> direction. In the path 3, the I_O migrates to an adjacent octahedral site with an energy barrier of 0.96 eV. The energy difference between these paths is about 0.38 eV. A main reason for this is due to the different geometries of the saddle states, leading to quite different energies for migration.

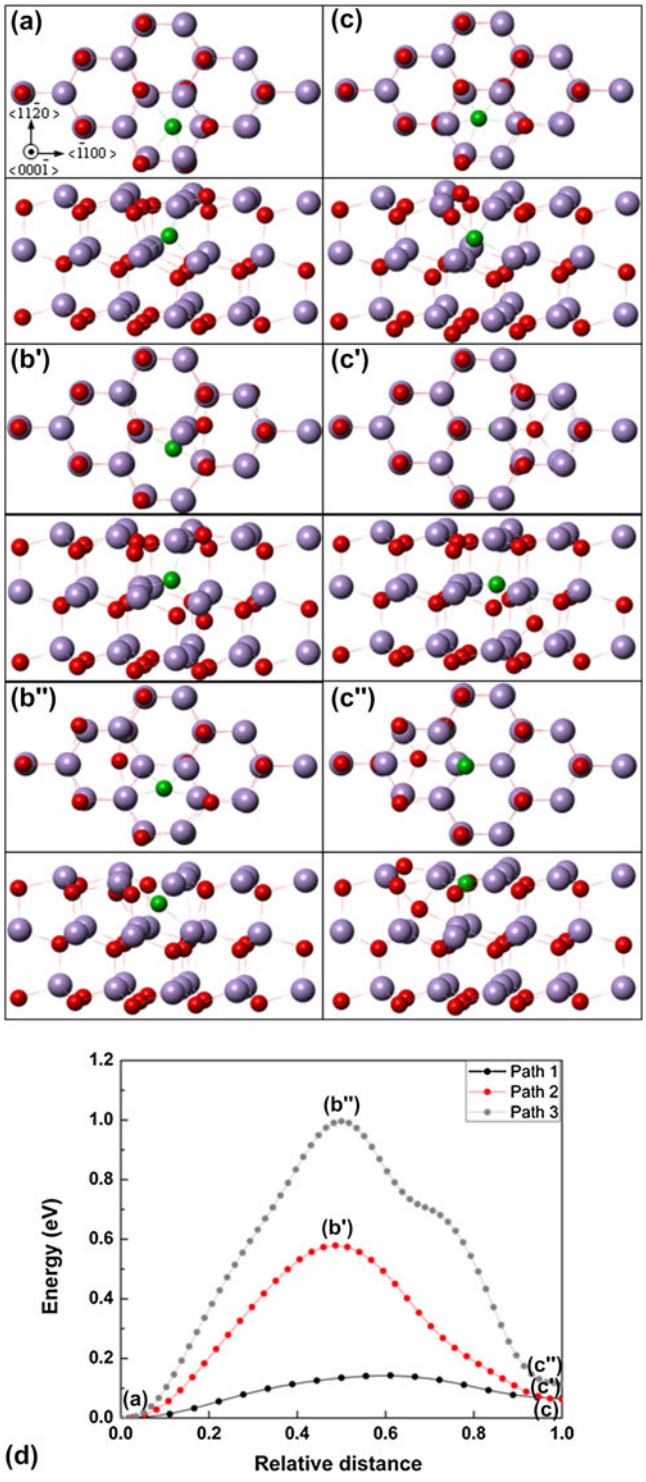


FIG. 4. Migration paths and the corresponding energy paths of an oxygen interstitial. (a) Starting configuration, (b′) and (b′′) saddle points, (c), (c′), and (c′′) final configurations, and (d) the calculated energy barriers along path 1 (a→c), path 2 (a→b′→c′), and path 3 (a→b′′→c′′). The transition to the nonsymmetric configuration requires the lowest energy barrier. The green sphere represents the initial oxygen interstitial.

E. Migration of interstitial–vacancy pair

As mentioned above, the low energy barrier of an oxygen interstitial allows it to diffuse at a low temperature. Here, we investigate the migration of an interstitial–vacancy pair (I_O–V_{Zn}) consisting of an octahedral oxygen interstitial and a single zinc vacancy, to explore how a vacancy affects the migration behavior of an I_O. Five possible migration paths and saddle points are determined by running 100 dimer searches. Figure 5 shows the first step of four migration paths and the MEPs for the I_O–V_{Zn} pair. As demonstrated in Fig. 5, the migration of the I_O–V_{Zn} pair can be considered as either I_O migration or zinc atoms

https://doi.org/10.1557/jmr.2012.153 Published online by Cambridge University Press

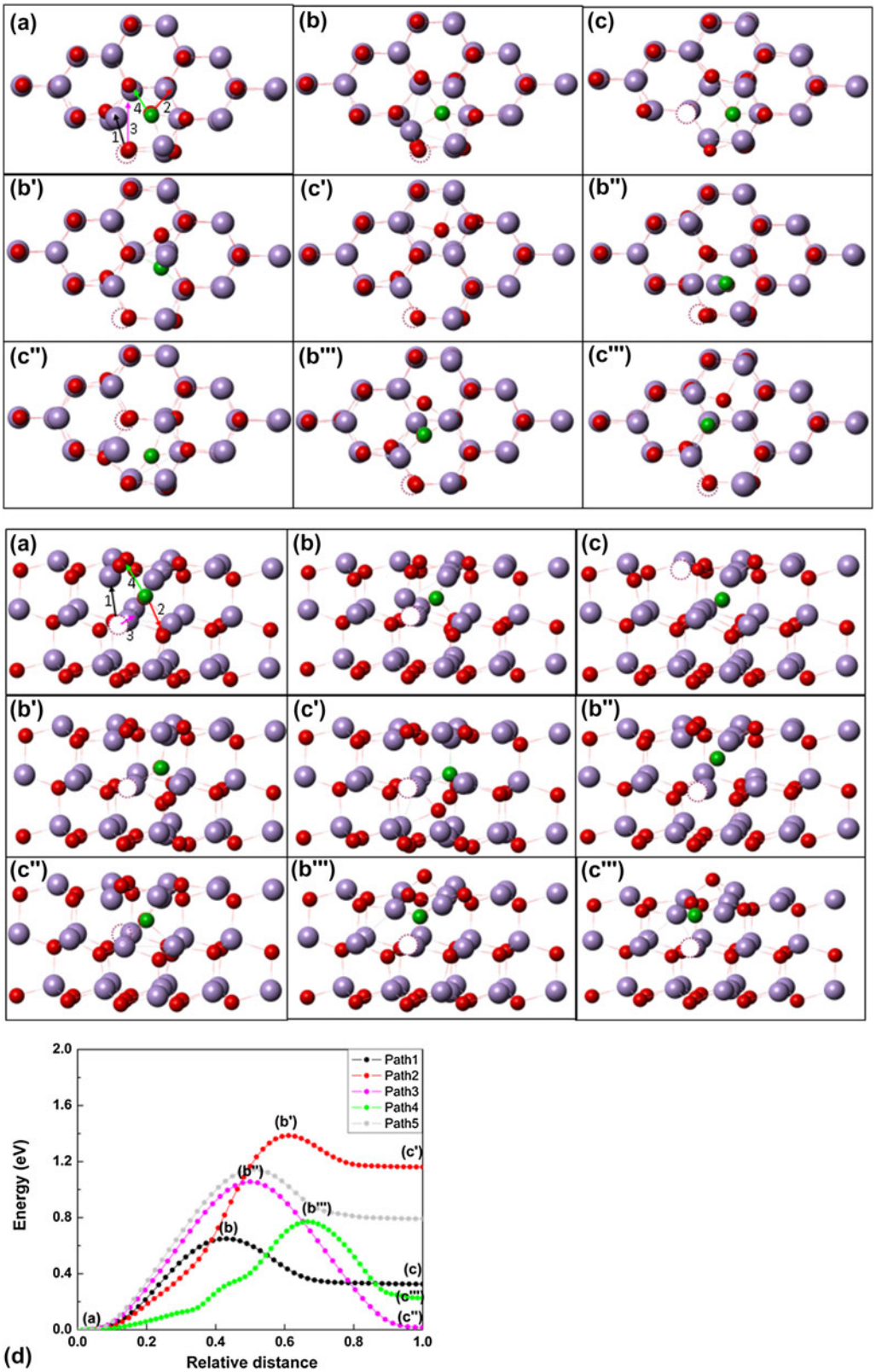


FIG. 5. The first step of four possible migration processes and the MEPs for an I_O–V_{Zn} pair consisting of an O interstitial (green atom) and a Zn vacancy (the dotted light purple circle). Path 1 (a→b→c) and path 3 (a→b′′→c′′) show the migrations of the V_{Zn} in the I_O–V_{Zn} pair. Path 2 (a→b′→c′) and path 4 (a→b′′′→c′′′) illustrate the migrations of the I_O in the I_O–V_{Zn} pair. (d) The calculated energy paths along path 1, path 2, path 3, path 4, and path 5. Also, path 5 in (d) corresponds to the energy barrier for the first step of the multistep migration process in Fig. 6. Upper panels show top views, while lower panels show side views. In the first frame, the respective paths are labeled.

https://doi.org/10.1557/jmr.2012.153 Published online by Cambridge University Press

hopping to and from the vacancy. A nearest neighbor zinc atom in the adjacent basal plane moves into the vacancy site (see a→b→c in Fig. 5), which needs to overcome an energy barrier of 0.65 eV. Compared to the out of plane motion of the V_{Zn} migration discussed in Sec. III. A, the energy path of path 1 (a→b→c) is distorted, which is affected by the nearby I_O. The energy barrier largely decreases from 1.35 to 0.65 eV, and the energy difference between the initial and final states in Fig. 5(d) is about of 0.33 eV. Also the nearest neighbor zinc atom in the same basal plane of V_{Zn} could jump into the vacancy position (see a→b″→c″ in Fig. 5). The calculated migration energy for path 3 (a→b″→c″) is only 1.05 eV, which is 0.72 eV lower than that for a single V_{Zn} transition. It indicates that the mobility of V_{Zn} could be enhanced in the presence of the I_O.

Compared to the mobility of oxygen interstitial discussed in Sec. III. D, it is unexpected for the I_O in the I_O–V_{Zn} pair to migrate rather slowly. The kick-out mechanism is still a dominant mechanism for the migration of the I_O in the I_O–V_{Zn} pair. The I_O replaces the nearest neighbor oxygen atom and then pushes it to form a new octahedral interstitial (see a→b′→c′ and a→b‴→c‴ in Fig. 5). Due to the anisotropic diffusion nearby the V_{Zn}, the energy barriers for path 2 (a→b′→c′) and path 4 (a→b‴→c‴) are 1.38 and 1.14 eV, respectively. Compared to a single oxygen interstitial, the existence of zinc vacancy restricts the I_O migration in the I_O–V_{Zn} pair.

Figure 6 provides an example to illustrate a possible multistep migration process. The final state of the minimum energy path is used as the initial atomic configuration for subsequent dimer searches and this process is repeated until a migration process of the cluster completes. There are two steps needed to complete a migration process of the I_O–V_{Zn} pair and the corresponding energy barrier is illustrated in Fig. 6. In this migration process, the nearest neighbor oxygen atom migrates into an adjacent octahedral interstitial via the kick-out mechanism (see a→b→c in Fig. 6) with an energy barrier of 0.77 eV [see a→b→c in Fig. 6(f)], and then, the out-of-plane Zn atom hops into the vacancy position (see c→d→e in Fig. 6) overcoming an energy barrier of 1.07 eV [see c→d→e in Fig. 6(f)]. Briefly, the I_O–V_{Zn} pair needs to overcome an energy barrier of 1.07 eV following this path. The set of movements separates the I_O–V_{Zn} pair a distance of almost 5 Å.

It is of interest to further consider the migration behavior of zinc vacancy–interstitial Frenkel pair consisting of a V_{Zn} and I_{Zn} with different separation distances, which will be discussed in details below. After the atomic relaxation of the starting configuration, we find that the pair is recombined even for a long distance of 3.8 Å between V_{Zn} and I_{Zn}. The long-range Coulombic interaction

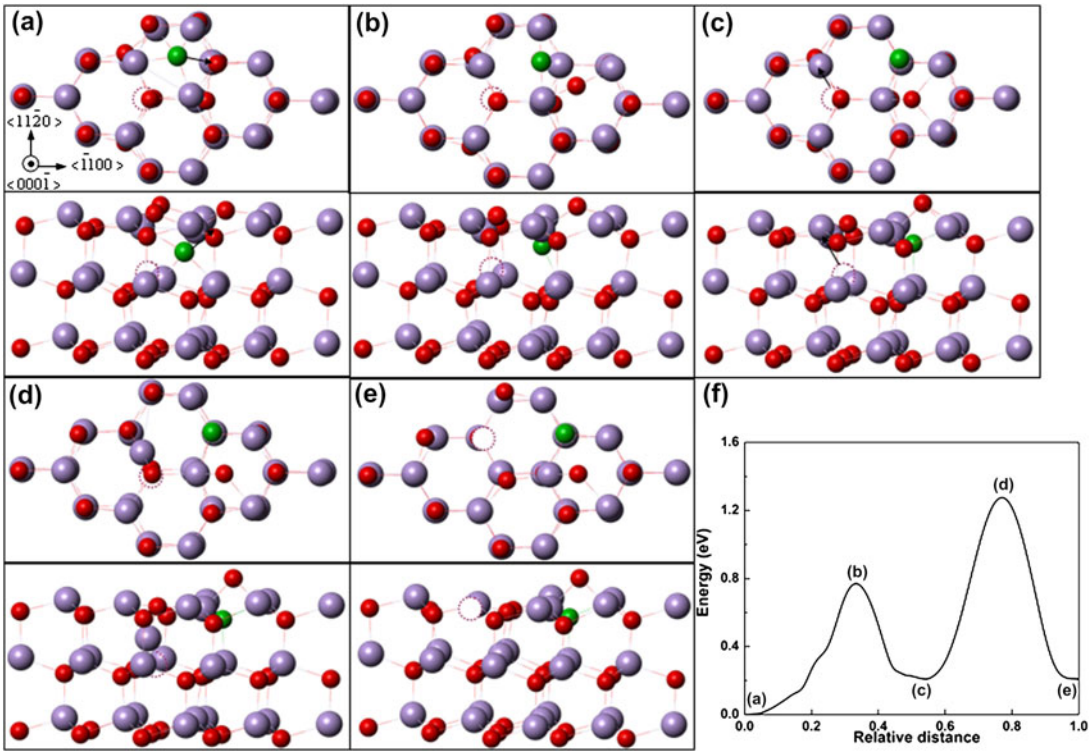


FIG. 6. The multistep migration process of an I_O–V_{Zn} pair. Lower right panel shows the migration energy path of the I_O–V_{Zn} pair, where the migration process from c→e leads to the highest energy barrier. The black arrows in (a) and (c) indicate the defect movements in the next frame.

https://doi.org/10.1557/jmr.2012.153 Published online by Cambridge University Press

is responsible for the strong attraction between the vacancy and the interstitial. We also performed a simulation when the distance between the vacancy and the interstitial is initially at least 3.2 Å, finding the migration of an oxygen Frenkel pair gives the result similar to the case of zinc Frenkel pair discussed above.

IV. CONCLUSIONS

We have performed a detailed investigation of the migration paths and determined the corresponding MEPs of vacancies, interstitials, and an interstitial–vacancy pair in zinc oxide using the dimer method. A difference between the in-plane and out-of-plane migrations for zinc and oxygen vacancies is as large as 0.5 eV. Based on the calculated migration barriers for zinc and oxygen vacancies, we predict that the migration of vacancies in ZnO is anisotropic. Zinc and oxygen interstitials migrate via the kick out mechanism with rather low energy barriers, which is in agreement with experimental observations and first-principles study. In addition, an interstitial–vacancy pair containing an octahedral oxygen interstitial and a single zinc vacancy exhibits more complex migration behaviors. In the case of an interstitial–vacancy pair, the migration barrier of the zinc vacancy is 0.72 eV lower than that for a single V_{Zn} transition, whereas an oxygen interstitial diffuses more difficult, as compared to a single I_O transition. Obviously, the influence of other defects on the migration behaviors of defect cluster is notable. Finally, a possible migration path of the I_O–V_{Zn} pair indicates that the I_O or V_{Zn} successive jumps can lead to the defect clusters migration, which can provide a guide to probe the migration behaviors of defect clusters under nonequilibrium conditions.

ACKNOWLEDGMENT

This research was supported by the National Natural Science Foundation under Contract No. 11147165. F. Gao was supported from the Division of Materials Sciences and Engineering, Office of Basic Energy Sciences, U.S. Department of Energy under Contract DE-AC05-76RL01830.

REFERENCES

1. T. Dietl and H. Ohno: Ferromagnetic III–V and II–VI Semiconductors. *MRS Bull.* **28**, 714 (2003).
2. S.K. Kamilla and S. Basu: New semiconductor materials for magnetoelectronics at room temperature. *Bull. Mater. Sci.* **25**, 541 (2002).
3. F. Oba, M. Choi, A. Togo, and I. Tanaka: Point defects in ZnO: An approach from first principles. *Sci. Technol. Adv. Mater.* **12**, 034302 (2011).
4. M. Nogueira, A. Sabioni, and W. Ferraz: Zinc self-diffusion in ZnO. *Defect Diffus. Forum* **237–240**, 163 (2005).
5. M.A.d.N. Nogueira, W.B. Ferraz, and A.C.S. Sabioni: Diffusion of the ^{65}Zn radiotracer in ZnO polycrystalline ceramics. *Mater. Res.* **6**, 167 (2003).
6. D.C. Look, B. Claflin, Y.I. Alivov, and S.J. Park: The future of ZnO light emitters. *Phys. Status Solidi A* **201**, 2203 (2004).
7. L.S. Vlasenko and G.D. Watkins: Optical detection of electron paramagnetic resonance for intrinsic defects produced in ZnO by 2.5-MeV electron irradiation *in situ* at 4.2 K. *Phys. Rev. B* **72**, 035203 (2005).
8. L.S. Vlasenko: Magnetic resonance studies of intrinsic defects in ZnO: Oxygen vacancy. *Appl. Magn. Res.* **39**, 103 (2010).
9. A. Janotti and C.G. Van de Walle: New insights into the role of native point defects in ZnO. *J. Cryst. Growth* **287**, 58 (2006).
10. P. Erhart and K. Albe: Diffusion of zinc vacancies and interstitials in zinc oxide. *Appl. Phys. Lett.* **88**, 201918 (2006).
11. P. Erhart and K. Albe: First-principles study of migration mechanisms and diffusion of oxygen in zinc oxide. *Phys. Rev. B* **73**, 115207 (2006).
12. G. Henkelman and H. Jónsson: Improved tangent estimate in the nudged elastic band method for finding minimum energy paths and saddle points. *J. Chem. Phys.* **113**, 9978 (2000).
13. G. Henkelman and H. Jónsson: A dimer method for finding saddle points on high dimensional potential surfaces using only first derivatives. *J. Chem. Phys.* **111**, 7010 (1999).
14. L.J. Munro and D.J. Wales: Defect migration in crystalline silicon. *Phys. Rev. B* **59**, 3969 (1999).
15. F. Gao, G. Henkelman, W.J. Weber, L.R. Corrales, and H. Jónsson: Finding possible transition states of defects in silicon-carbide and alpha-iron using the dimer method. *Nucl. Instrum. Methods Phys. Res., Sect. B* **202**, 1 (2003).
16. D. Chen, W.Y. Hu, F. Gao, H.Q. Deng, and L.X. Sun: Tungsten cluster migration on nanoparticles: Minimum energy pathway and migration mechanism. *Eur. Phys. J. B* **80**, 31 (2011).
17. D. Chen, F. Gao, W.Y. Hu, S.Y. Hu, D. Terentyev, H.L. Heinisch, C.H. Henager, and M.A. Khaleel: Migration of Cr-vacancy clusters and interstitial Cr in α-Fe using the dimer method. *Phys. Rev. B* **81**, 64101 (2010).
18. W. Smith and T.R. Forester: DL_POLY_2.0: A general-purpose parallel molecular dynamics simulation package. *J. Mol. Graphics* **14**, 136 (1996).
19. A.J. Kulkarni, M. Zhou, and F.J. Ke: Orientation and size dependence of the elastic properties of zinc oxide nanobelts. *Nanotechnology* **16**, 2749 (2005).
20. D.J. Binks and R.W. Grimes: Incorporation of monovalent ions in ZnO and their influence on varistor degradation. *J. Am. Ceram. Soc.* **76**, 2370 (1993).
21. L. Dai, W.C.D. Cheong, C.H. Sow, C.T. Lim, and V.B.C. Tan: Molecular dynamics simulation of ZnO Nanowires: Size effects, defects, and super ductility. *Langmuir* **26**, 1165 (2009).
22. A. Janotti and C.G. Van de Walle: Native point defects in ZnO. *Phys. Rev. B* **76**, 165202 (2007).
23. M.G. Wardle, J.P. Goss, and P.R. Briddon: Theory of Fe, Co, Ni, Cu, and their complexes with hydrogen in ZnO. *Phys. Rev. B* **72**, 155108 (2005).
24. G. Huang, C. Wang, and J. Wang: First-principles study of diffusion of oxygen vacancies and interstitials in ZnO. *J. Phys. Condens. Matter* **21**, 195403 (2009).

https://doi.org/10.1557/jmr.2012.153 Published online by Cambridge University Press